PII: S0032-3861(96)00859-2

Polymer Vol. 38 No. 12, pp. 2885–2891, 1997

0032-3861/97/$17.00 + 0.00

Aqueous solution properties of oligo- and poly(ethylene oxide) by static light scattering and intrinsic viscosity

Seigou Kawaguchi*, Genji Imai†, Junto Suzuki‡, Akira Miyahara§, Toshiaki Kitano|| and Koichi Ito*
Department of Materials Science, Toyohashi University of Technology, Tempaku-cho, Toyohashi, 441 Japan
(Received 1 July 1996; revised 5 August 1996)

Conformational properties of ethylene glycol, oligo-, and poly(ethylene oxide) ranging in weight-average molecular weight (M_w) from 62 to 1.1×10^7 have been studied by static light scattering and viscometry in salt-free and 0.45 M K_2SO_4 water and in benzene. Above $M_w = 6 \times 10^3$, intrinsic viscosity ($[\eta]$) and z-average square radius of gyration ($\langle S^2 \rangle_z$) of PEO in a salt-free solution at 25°C, $[\eta] = 4.33 \times 10^{-4} M_w^{0.67_9}$ dl g^{-1} and $\langle S^2 \rangle_z = 4.08 \times 10^{-18} M_w^{1.1_6}$ cm^2, respectively. The second virial coefficient is positive in water at 25°C but one order of magnitude smaller than reported by Devanand *et al.* (*Macromolecules*, 1991, **24**, 5943). A θ-temperature for PEO in 0.45 M K_2SO_4 aqueous solution is determined to be 34.5°C and above $M_w = 4 \times 10^2$, $[\eta]$ and $\langle S^2 \rangle_z$ follow the power laws for an unperturbed polymer chain. The characteristic ratio (C_∞) of PEO is 5.2 ± 0.1. 9.3 Å was determined for the persistence length and 8.7 Å^{-1} for the molar mass per unit contour length of a PEO chain, based on the helical wormlike touched-bead model. The PEO chain in water behaves as a flexible polymer with a relatively large hydrodynamic diameter (9 Å) because of the hydration of the PEO chain. © 1997 Elsevier Science Ltd.

(Keywords: poly(ethylene oxide); light scattering; intrinsic viscosity)

INTRODUCTION

Poly(ethylene oxide) (PEO) is a simple and representative linear amphiphilic polymer with interesting behaviour both in solution and in the solid state[1–3]. It dissolves not only in a large number of organic solvents but also in water. Because of the fundamental importance and wide applications[4,5], many authors have studied its solution properties. The studies have been carried out both in the polymer and colloid field but the behaviour of PEO in water has been less quantatively understood, when compared with that of, say, polystyrene (PS) in organic solvents. Unusual phenomena observed in water have been exclusively ascribed to the specificity of water as a solvent.

Studies on PEO solution properties are concerned with three subjects. First, PEO exhibits in water both upper and lower critical solution temperature phenomena (UCST and LCST). Several models have been proposed, including an entropic model due to structured water, hydrogen bond formation between polymer segments and solvent, and a conformation model[6]. The first two models are the result of specific water structuring along a PEO backbone[3]. There are data suggesting that two water molecules are associated with each ethylene oxide monomer unit and the diffusion coefficient of the water near a chain is substantially lower than in bulk water[7,8]. The phase separation, however, also takes place in a non-hydrogen-bonding solvent such as *t*-butyl acetate[9]. This shows that water specificity as a solvent is not necessarily a key factor in this behaviour. Several spectroscopic studies using Raman[10–12] and X-ray scattering[13], n.m.r.[14–16], and dielectric constant measurements[17] have shown that the conformation around the central OC-CO bond varies depending on the polarity of the surroundings. Recently, the local conformation of the PEO chain has caused controversy[18].

The second problem concerns the tendency of PEO to aggregate in solution. The aggregation in various solvents has been reported by several research groups. For example, Polik and Burchard[19] reported that PEO chains aggregate significantly in water over a wide temperature range from 20 to 90°C. Zhow and Brown[20] also reported that the PEO molecules aggregate in methanol at room temperature. They observed a significant downturn in the angular dependence of the light scattering, indicating the presence of some aggregates in *good solvents*. However, Kato *et al.*[21] reported that PEO does not aggregate in water from the measurements of dynamic and static light scattering, and viscometry. Quite recently, static and dynamic light

---

* To whom correspondence should be addressed

† Present address: Kansai Paint Co., Ltd, 4-17-1, Higashiyawata, Hiratsuka, 254 Japan

‡ Present address: Dai-nichi Seika Co., Ltd, 4-3-35, Ryoke, Kawaguchi, 322 Japan

§ Present address: Nippon Kagakuhakko Co., Ltd, 2-19-17, Hakataekimae, Hakataku, Fukuoka, 812 Japan

|| Present address: Polyplastics Co., Ltd, 973 Miyajima, Fuji, 416 Japan

scattering measurements by Devanand *et al.*[22] and Kinugasa *et al.*[23] found that PEO molecules do not aggregate in water, methanol, and acetonitrile at room temperature, when the solutions are meticulously prepared. The second virial coefficients reported by Devanand *et al.*[22], however, are of unreasonably large values, when compared with those of PS and poly(methyl methacrylate) (PMMA) with corresponding molecular weights in good solvents.

The third subject of interest is the complexation of PEO with small cations in organic solvents. Lundberg *et al.*[24] reported that PEO chains behave like a polyelectrolyte in methanol when potassium iodide is added. In water, however, the complexation may not take place but the solubility power of water for PEO chains may decrease with increasing salt concentration (C_s). Here, we chose 0.45 M K_2SO_4 aqueous solution as a θ-solvent.

Over the past decade, we have been studying the polymerization behaviour of polymerizable PEO macromonomers from the viewpoint of their amphiphilic character, in order to prepare multiphase well defined graft copolymers[25]. When one analyses the polymerization behaviour and the solution properties of the resulting graft copolymers, comblike polymers[26], and latex surface graft copolymers[27,28], an understanding of the conformational properties of a PEO chain is essential as a reference.

The present paper reports conformational properties of the PEO chain in water or benzene. We measured $[\eta]$ and $\langle S^2 \rangle_z$ of the PEO samples with a weight-average molecular weight (M_w) ranging from 62 (ethylene glycol) to 1.1×10^7 and compared it with the draft reported. The θ-temperature was determined and the data obtained under this condition were compared with the helical worklike touched-bead model (HW) developed by Yamakawa and his coworkers[29]. The characteristic parameters of PEO chains in water including the persistence length, characteristic ratio, and hydrodynamic diameter were determined and discussed.

EXPERIMENTAL

Materials and preparation of solutions

Five samples below $M_n = 750$ were purchased from Kishida Chemical Co., Japan. The samples, PEO-2K, 4K, 5K and 20K were supplied from Nakarai Chemical Co., Japan, and PEO-10K was donated by the Takemoto Oil & Fat Co., Japan. The samples of the SE-n series were from the Tosoh Co., Japan and PEO-15H and -18H from the Seitetsu Chemical Co., Japan. The samples below $M_n = 400$ were used without further purification. The samples with molecular weights between 750 and 88×10^4 were reprecipitated three times by pouring their benzene solutions into excess hexane. The precipitated samples were filtered off, washed with hexane, and freeze-dried from benzene, and dried *in vacuo* to constant weight. PEO-18H and -15H with broad molecular weight distributions were fractionated with benzene–isooctane and purified by the above procedures. Air in the sample containers was replaced with argon and the samples kept in a freezer. All the samples were again dried *in vacuo* at least for 24 h at room temperature just before preparation of the solution. K_2SO_4 (Kishida) was dried *in vacuo* at 80°C for 24 h just before use. Water purified with a Millpore Milli Q purification system was used in all experiments. H.p.l.c. grade benzene (Kishida) for optical calibration in light scattering experiment and for viscometry was used as received. In viscometry, 0.1 vol% of allyl alcohol (Kishida) was added to the water, to avoid oxidation of PEO[30,31]. Time-dependent viscosity measurements revealed no chain breaking even for the sample above $M_w = 10^6$.

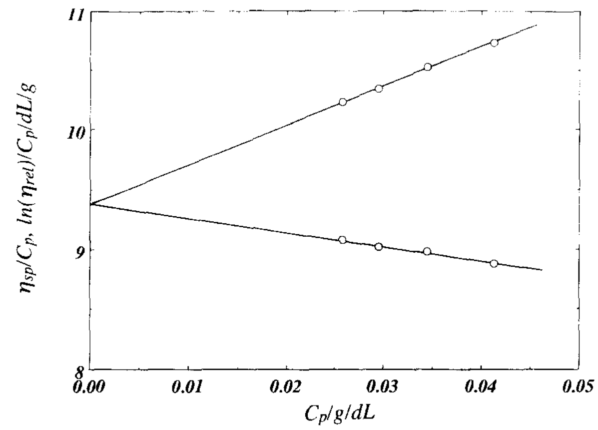

Figure 1 Plots of η_{sp}/C_p (upper) and $\ln(\eta_{rel})/C_p$ (lower) of PEO-18HD salt-free aqueous solution against polymer concentration (C_p) at 25°C

All the solutions except for the θ-solvent were prepared by standing in the dark without shaking at room temperature at least for 3 days. All solutions were prepared gravimetrically, and their polymer mass concentrations C_p (g ml^{-1}) were calculated.

Measurements

V.p.o. Vapour pressure osmometry (v.p.o.) was run with a molecular weight apparatus from Corona Electric Co., Ltd, Type 117 at 45°C. Thiophene-free benzene was used and the instrument was calibrated with 1,2-diphenylethane (Kishida).

Viscometry. Viscometry measurements were carried out using a four-bulb low-shear capillary viscometer for molecular weights PEO higher than 10^5 and a conventional capillary viscometer of the Ubbelohde type for the lower molecular weight samples. The Huggins plot[32] and the Fuoss–Mead plot[33] were combined to determine $[\eta]$. A typical example is shown in *Figure 1*.

G.p.c. Aqueous gel permeation chromatography (g.p.c.) was carried out at 25°C, using a HLC-8020 (Tosoh Co. Ltd), fitted with three columns (TSK-G-6000PW$_{XL}$, 4000PW$_{XL}$, and 2500PW$_{XL}$) and a refractive index detector. The chromatographic solvent (1 ml min^{-1}) was water containing a small amount of sodium azide. The elution volume was calibrated with nine PEO standard samples ($150 < M_w < 2.26 \times 10^6$).

Refractive index increment. Excess refractive indices of PEO solution in the presence and absence of K_2SO_4 were measured using a differential refractometer, RM-102 from Otsuka Electronics, Co. Ltd and RF-600 from C. N. Wood Mfg. Co., Ltd. The refractive index increment (dn/dc) for a salt-free aqueous solution of PEO with $M_w = 2.24 \times 10^4$ was 0.132_8 ml g^{-1} at $\lambda =$ 632.8 nm 25°C. The dn/dc values for undialysed PEO ($M_w = 2.24 \times 10^4$) solution containing 0.45 N K_2SO_4 were 0.119 ml g^{-1} at 33.0°C and 0.124 ml g^{-1} at 36.0°C.

Table 1 Results from v.p.o., g.p.c., light scattering, and viscosity measurements of ethylene glycol, oligo- and poly(ethylene oxide) samples

Code	$10^{-3}M_n$ v.p.o.	$10^{-4}M_w$ LS	M_w/M_n^b g.p.c.^{b}	$[\eta]_{H_2O}$ $(dl\,g^{-1})^c$	$[\eta]_\theta$ $(dl\,g^{-1})^d$	$[\eta]_{benzene}$ $(dl\,g^{-1})^e$	$10^{12}\langle S^2\rangle_{z H_2O}$ $(cm^2)^c$	$10^{12}\langle S^2\rangle_{z\theta}$ $(cm^2)^d$
EG	0.0621^a		1.00^a	0.022_1	0.021_4			
DEG	0.106^a		1.00^a	0.023_7	0.024_2			
TEG	0.152^a		1.00^a	0.027_7	0.028_8			
PEO–0.4K	0.40		1.0_6	0.040_0	0.034_0	0.028_3		
PEO-0.75K	0.75		1.1_0	0.055_0	0.054_8	0.039_0		
PEO-2K	1.9_4		1.0_7	0.087_0	0.077_0	0.073_6		
PEO-4K	3.8_0		1.0_5	0.130	0.105	0.095_1		
PEO-5K	5.1_9		1.0_9	0.152	0.119			
PEO-10K	$12._2$		1.0_9		0.181	0.219		
PEO-20K		2.2_4	1.1_5	0.395	0.253	0.376		
SE8		8.6_0	1.1_0	1.02				
SE15		$15._0$	1.0_8	1.52				
SE15		$17._3$	1.1_3	1.47	0.715	1.45_5	4.87	
SE30		$32._1$	1.0_8	2.15				
SE30		$34._8$	1.0_5	2.61	0.968	2.26	10.6	4.41
SE70		$53._8$	1.1_0	3.60	1.20	3.06	17.1	6.77
SE70		$61._1$	1.2_8	3.33			25.2	
SE150		$86._8$	1.1_7	4.74	1.52	4.93	28.1	11.1
SE150		$88._2$	1.2_5	4.33			32.0	
PEO-18HD		22_6	1.2_0	9.33		9.33	92.7	
PEO-15HC		44_6		15.1			226	
PEO-18HC		110_0		25.7			1450	

[a] Calculated from the molecular formula
[b] Calibrated with a series of PEO samples
[c] At 25°C
[d] In 0.45 M K_2SO_4 solution at 34.5°C
[e] At 25°C

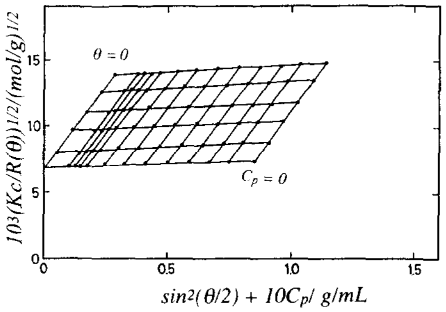

Figure 2 Berry square-root plots for PEO-20K in salt-free aqueous solution at 25°C

Light scattering Static light scattering measurements were run with a modified LS-601 (Union Gikken Co., Ltd) equipped with a vertically polarized light of a 10 mW He–Ne laser of 632.8 mm as an incident beam. For optical purification, the aqueous solution was filtered slowly and directly into light scattering cells using a microfeeder. The filters used were cellulose acetate membrane filters (0.2–1.0 μm) with a 25 mm diameter. The water used for light scattering measurement was three times filtered. The Rayleigh ratio $R(\theta)$ of the scattered light was based on the Rayleigh ratio $R_B(90) = 11.84 \times 10^{-6}\,cm^{-1}$ of pure benzene at a wavelength (λ_0) of 632.8 nm[34].

Scattered intensity data at angles (θ) were analysed by Berry square-root plots

$$\left(\frac{KC_p}{R(\theta)}\right)^{\frac{1}{2}} = \left[\frac{1}{M_w}\left(1 + \frac{16\pi^2 n_0^2}{3\lambda_0^2}\langle S^2\rangle_z \sin^2\left(\frac{\theta}{2}\right) + 2A_2 M_w C_p + \dots\right)\right]^{\frac{1}{2}} \quad (1)$$

where n_0 is the refractive index of the solvents and A_2, the second virial coefficient, and K is the optical constant given as $K = 4\pi^2 n_0^2 (dn/dc)^2/(\lambda_0^4 N_A)$ with Avogadro's number N_A.

RESULTS AND DISCUSSION

Salt-free aqueous solution

Figure 2 shows Berry square-root plots for PEO-20K in salt-free aqueous solution at 25°C. It is seen that it has a normal form without any downturn in low θ and gives a reasonable M_w value, suggesting that no aggregates exist in water at 25°C. Such results were obtained for all samples we examined by light scattering. Thus, it is fair to say that PEO does not aggregate in water at 25°C. For samples with a molecular weight below 2×10^4, the number-average molecular weight (M_n) is determined by v.p.o. measurements and for the higher molecular weight samples M_w is determined by light scattering measurements. The molecular characteristics of the PEO samples we used are listed in *Table 1*. The polydispersity index (M_w/M_n) determined from g.p.c. shows that the samples, except for PEO-15HC and PEO-18HC have relatively narrow, molecular weight distributions.

The values of $[\eta]$ determined for PEO in salt-free solution at 25°C are listed in *Table 1* and the double logarithmic plot (open circles) against M_w is shown in *Figure 3*. It can be seen that the present data are in good agreement with those (triangles) reported by Kato[21]. For $62 < M_w < 6 \times 10^3$ the slope of log $[\eta]$ against log M_w gradually increases with increasing M_w and for $10^3 < M_w < 6 \times 10^3$ it is nearly 0.5. For $M_w > 6 \times 10^3$, the slope is almost constant giving

$$[\eta] = 4.33 \times 10^{-4} M_w^{0.67_9} \quad dl\,g^{-1} \quad (2)$$

The values of $\langle S^2\rangle_z$ in salt-free solution at 25°C are also summarized in *Table 1* and the double logarithmic

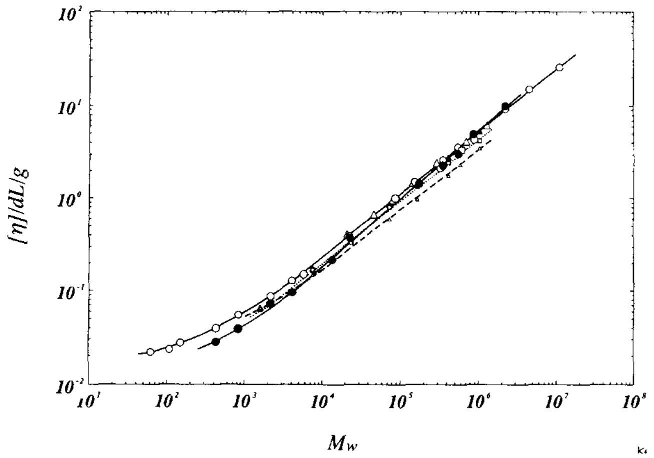

Figure 3 Molecular weight dependence of [η] for PEO in salt-free solution at 25°C (○) and in benzene at 25°C (●). The literature data in the various solvents are shown for comparison, (△) in water at 25°C[21], (▲) in benzene at 25°C[35], (□) in CCl_4 at 25°C[35], (□) in acetone at 25°C[35]

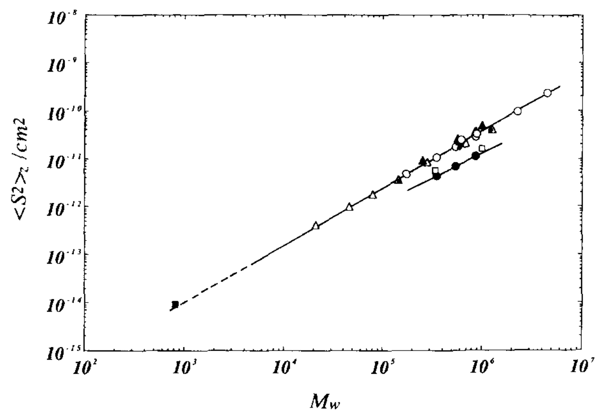

Figure 4 Molecular weight dependence of $\langle S^2\rangle_z$ for PEO in salt-free solution at 25°C (○) and in 0.45 M K_2SO_4 solution at 34.5°C (●). The data reported are also plotted for comparison, (△) in water at 25°C[21], (□) in water at 25°C[23], (▲) in water at 30°C[22], (●) in methanol at 25°C[20], and (■) in acetonitrile[41]

plot against M_w, is shown in *Figure 4*, together with the data reported by several groups. The present data are in good agreement with those at 30°C reported by Devanand *et al.*[22] and those in MeOH at 25°C by Zhou *et al.*[20], but slightly higher than those in water at 25°C by Kinugasa *et al.*[23]. Except for the last data, the results are fitted by

$$\langle S^2\rangle_z = 4.08\times10^{-18} M_w^{1.1_6} \quad \text{in cm}^2 \qquad (3)$$

These power laws relating [η] and $\langle S^2\rangle_z$ with M_w above about $M_w = 6\times10^3$ in water at 25°C show that a PEO chain assumes an expanded random coil conformation by an excluded-volume effect in a typical good solvent.

Comparison of PEO's [η] in water with those in organic solvents

The [η] values determined in benzene at 25°C are listed in *Table 1* and plotted against M_w, as shown in *Figure 3*. The data of [η] reported by Beech and Booth[35] are also plotted for comparison. There are two interesting points to be noted in this figure. First above $M_w = 1\times10^4$, the values of [η] in benzene approach those in water with increasing M_w. Above $M_w = 5\times10^3$, the slope of a plot of log [η] against log M_w is 0.69_9 in benzene, 0.66_2 in CCl_4, and 0.61_2 in acetone, respectively. Thus, benzene is the best solvent for PEO at 25°C among these. Second, for $M_w < 1\times10^4$, the values of [η] in water are larger than those in the other organic solvents. This may be due either to an increase of the apparent hydrodynamic volume of PEO by hydration as will be discussed later, or to a difference in the local conformation. Below $M_w = 5\times10^3$, the slope in organic solvents also increases gradually with increasing M_w and to an almost constant value, just like the result observed in salt-free water at 25°C.

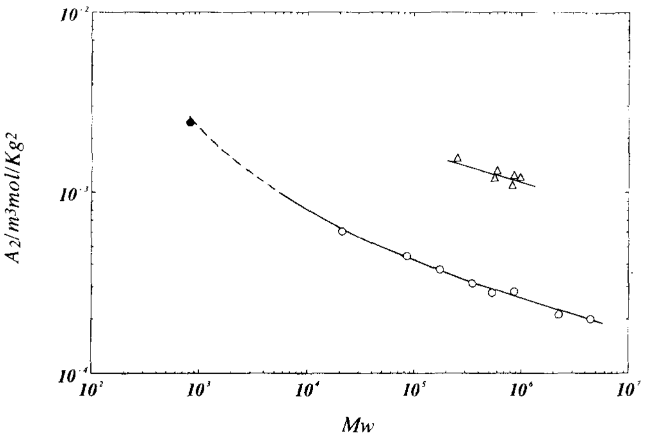

Figure 5 Molecular weight dependence of second virial coefficient (A_2) of PEO in salt-free aqueous solution at 25°C (○). The A_2 at 30°C (△)[22] and (●) in CH_3CN[41] are shown for comparison

Second virial coefficients

Figure 5 shows a double logarithmic plot of A_2 at 25°C against M_w. The data in water at 30°C by Devanand *et al.*[22] are also shown for comparison. Two points to be noted in this figure are the difference in the absolute values and in the molecular weight dependence between them. At the same M_w, the present data at 25°C which are similar to those reported for PS[36] and PMMA[37] in good solvents, are one order of magnitude smaller than those at 30°C. Devanand *et al.* interpreted the enhanced coil–coil interaction in terms of the supposedly unusual ability of water molecules to pack into and swell the coils. In fact, Bailey and his coworkers reported that the exponent of the power law in M_w-dependence of the [η] is 0.78 at 30°C[38], 0.82 at 35°C[39], and 0.81 at 45°C[39], which are considerably higher than the present value (0.67_9) at 25°C. At this moment, we suspect that this big difference is due to a change in the water specificity with temperature. The studies about the influence of temperature on PEO chain conformation in water are now in progress.

The slope of A_2 against M_w in the present data in *Figure 5* slowly decreases with M_w. For M_w higher than 10^5:

$$A_2 = 3.7_2\times10^{-3} M_w^{-0.19\pm0.02} \quad \text{m}^3\,\text{mol}\,K_g^2 \qquad (4)$$

In the two-parameter theory, A_2 depends on a penetration function (Ψ), a universal function of an excluded volume parameter[40],

$$A_2 = \Psi \frac{4\pi^{3/2} N_A \langle S^2\rangle^{3/2}}{M^2} \qquad (5)$$

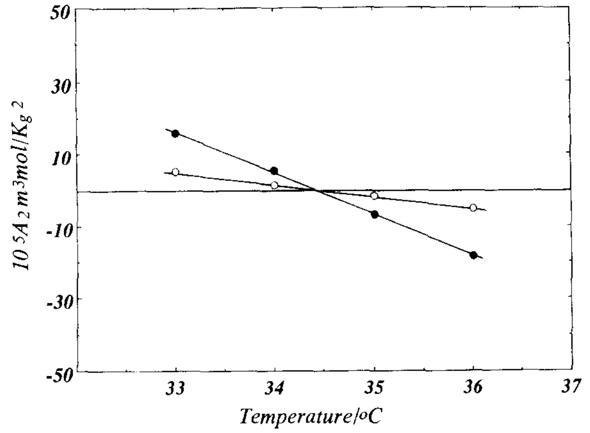

Figure 6 Temperature dependence of A_2 in 0.45 M K_2SO_4 solution of SE-70 (●) and SE-150 (○)

If Ψ asymptotically converges to a finite value at $M = \infty$, the equation is well known to predict $A_2 \sim M^{-0.2}$, in agreement with our data. Thus, the PEO chain behaves in water at 25°C like a conventional flexible linear polymer in a good solvent. We calculate Ψ using the variables determined in this work. The value for PEO-18HD is about 0.09, which is considerably smaller than the value (0.22–0.25)[40] found in PS and PMMA with a corresponding expansion factor ($\alpha^2 = \langle S^2 \rangle / \langle S^2 \rangle_\theta$).

θ-Temperature of 0.45 M K_2SO_4 solutions of PEO

To examine the solution behaviour in light of current theories, we need the θ-condition of PEO in aqueous solution. Two θ-solvent systems known for PEO are 0.45 M K_2SO_4 at 35°C[39] and 0.39 M $MgSO_4$ at 45°C[39]. We adopted the former. *Figure 6* shows plots of A_2 against temperature for the two PEO samples SE-70 and SE-150 in 0.45 M K_2SO_4. It is seen that A_2 vanishes at nearly the same temperature of 34.5°C.

The $\langle S^2 \rangle_z$ and $[\eta]$ in the θ-solvent are plotted against M_w in *Figures 4* and *7* (denoted by filled circles), and listed in *Table 1*. These plots are linear above $M_w = 400$, and by least squares we obtained

$$[\eta]_\theta = 1.57 \times 10^{-3} M_w{}^{0.50_4} \quad \mathrm{dl\,g^{-1}} \tag{6}$$

and

$$\langle S^2 \rangle_{z\theta} = 1.11 \times 10^{-17} M_w^{1.0_1} \quad \mathrm{cm^2} \tag{7}$$

The characteristic ratio (C_∞) of PEO in water defined by $C_\infty = (6\langle X^2 \rangle_\theta)/(n\overline{l^2})$ is calculated to be 5.2 ± 0.1, where n is the number of skeletal bonds, and $\overline{l^2}$ is the average of the square of their length ($= (l_{c-c}^2 + 2\,l_{c-o}^2)/3 = 2.14$ Å with $l_{c-c} = 1.53$ Å and $l_{c-o} = 1.43$ Å). The C_∞ value is in good agreement with that reported by several researchers[34,41,42], but remarkably smaller than 6.9–7.6 reported by Kugler *et al.*[43] and Vennemann *et al.*[44], and bigger than 4.0 reported by Flory[45].

The Flory–Fox viscosity factor (Φ_θ) for the θ-solvent is $2.4 \pm 0.1 \times 10^{23}$ mol^{-1} from the equation

$$\Phi_\theta = \frac{[\eta]_\theta M_w}{6^{3/2} \langle S^2 \rangle_\theta^{3/2}} \tag{8}$$

which is very close to the value, $2.5_5 \times 10^{23}$ mol^{-1} reported by Miyaki *et al.*[46] who investigated the PS–cyclohexane system, but slightly smaller than the recent value, $(2.79 \pm 0.08) \times 10^{23}$ mol^{-1}, reported by Konishi *et al.*[47]. In salt-free water at 25°C, the Φ is determined as $(1.3\text{–}1.9) \times 10^{23}$ in the M_w range we examined.

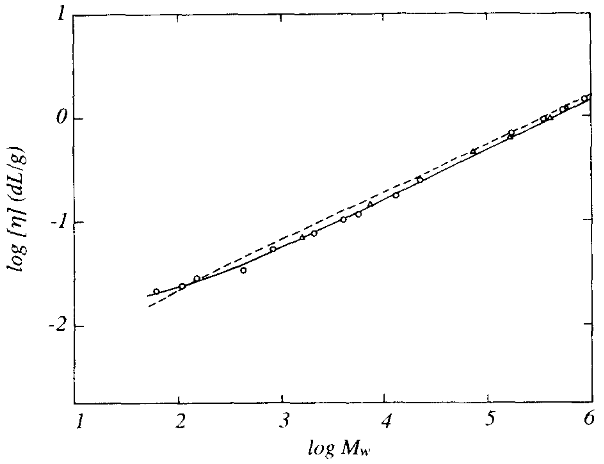

Figure 7 Comparison between the measured $[\eta]$ in 0.45 M K_2SO_4 aqueous solution at 34.5°C and helical wormlike touched-beads model. The dashed line is a theoretical curve with $\lambda^{-1}\kappa_0 = 2.4$, $\lambda^{-1} = 0.5$, $\lambda^{-1} = 12.6$ Å, $M_L = 7.9$ Å^{-1}, and $d_b = 3.2$ Å, and the solid line is one with $\lambda^{-1}\kappa_0 = 2.0$, $\lambda^{-1}\tau_0 = 4.0$, $\lambda^{-1} = 18._6$ Å, $M_L = 8.7_1$ Å^{-1}, and $d_b = 9.3$ Å. (○) Present work; (△) ref. 35

Comparison with the HW model

We apply the HW model without excluded volume, developed by Yoshizaki and Yamakawa[29], to our intrinsic viscosity data and determine several characteristic conformation parameters of a flexible PEO chain in water. According to the theory, $[\eta]$ is written as the sum of the solution $[\eta]_{KR}$ of the Kirkwood–Riseman equation and the contribution $[\eta]_E$ of the Einstein spheres,

$$[\eta] = [\eta]_{KR} + [\eta]_E \tag{9}$$

$[\eta]_E$ and $[\eta]_{KR}$ are given by

$$[\eta]_E = 5\pi N_A N d_b^3 / 12M \tag{10}$$

$$[\eta]_{KR} = \left(\frac{\langle S^2 \rangle}{\langle S^2 \rangle_{KP}} \right)^{3/2} [\eta]_{KR}^{KP} \Gamma(L, d_b\,;\, \kappa_0, \tau_0) \tag{11}$$

where N is the number of beads, d_b is a diameter of the bead, L is the HW chain contour length, κ_0 and τ_0 are related to curvature and torsional constants for a elastic wire. $\langle S^2 \rangle_{KP}$, $[\eta]_{KR}^{KP}$, and $\langle S^2 \rangle$, are given, respectively, by

$$\langle S^2 \rangle_{KP} = \frac{6}{L} - \frac{1}{4} + \frac{1}{4L} - \frac{1}{8L^2}(1 - e^{-2L}) \tag{12}$$

$$[\eta]_{KR}^{KP} = 6^{3/2} \Phi_\infty \langle S^2 \rangle_{KP}^{3/2} / M \Gamma_{KP}(L, d_b) \tag{13}$$

$$\begin{aligned} \langle S^2 \rangle = {} & \frac{{\tau_0}^2}{v^2} \langle S^2 \rangle_{KP} + \frac{k_0^2}{v^2} \left(\frac{L}{3r} \cos\phi - \frac{1}{r^2} \cos(2\phi) \right. \\ & + \frac{2}{r^3 L} \cos(3\phi) - \frac{2}{r^4 L^2} \cos(4\phi) \\ & \left. + \frac{2}{r^4 L^2} e^{-2L} \cos(nL + 4\phi) \right) \end{aligned} \tag{14}$$

where Φ_∞ is 2.870×10^{23}. v, r, and ϕ are defined by

$$v = (\kappa_0^2 + \tau_0^2)^{1/2} \tag{15}$$

$$= (4 + v^2)^{1/2} \tag{16}$$

$$\phi = \cos^{-1}(2/r) \tag{17}$$

The numerical function forms of Γ and Γ_{KP} are given in ref. 29 and all lengths are measured in units of λ^{-1}. Double-logarithmic plots of $[\eta]$ (in dl g^{-1}) against M is given by

$$\log[\eta] = \log(M[\bar{\eta}]/\Phi_\infty L) - \log(\lambda^2 M_L) - 2.542 \tag{18}$$

with

$$\log M = \log L - \log(M_L/\lambda) \tag{19}$$

where $[\bar{\eta}]$ is the reduced intrinsic viscosity calculated from the equations mentioned above and M_L is the shift factor defined as the molecular weight per unit contour length of the chain. The shape of the double logarithmic plot of $M[\bar{\eta}]/\Phi_\infty L$ changes only with the values of κ_0, τ_0, and d_b. Therefore, the quantities of M_L/λ and $\lambda^2 M_L$ may be determined from a best fit of the double-logarithmic plot of the theoretical $M[\bar{\eta}]/\Phi_\infty L$ against L to that of the observed $[\eta]$ against M. Fujii *et al.* determined the model parameters by applying the model to the experimental data of the mean-square dipole moment $\langle \mu^2 \rangle$ of PEO in benzene at 25°C[48]. The parameters are $\lambda^{-1}\kappa_0 = 2.4$, $\lambda^{-1}\tau_0 = 0.5$, $\lambda^{-1} = 12.0$ Å, and $M_L = 8.8$ Å^{-1}. First, we use the $\lambda^{-1}\kappa_0 = 2.4$ and $\lambda^{-1}\tau_0 = 0.5$, and determine λ^{-1}, M_L, and d_b from comparison with the present viscometric results. The best fit curve (broken lines) is shown in *Figure 7* and we obtain $\lambda d_b = 0.25$, $\log M_L/\lambda = 2.0$, and $\log \lambda^2 M_L = -1.3$. From these values, we determine $\lambda^{-1} = 12.6$ Å, $M_L = 7.9$ Å^{-1}, and $d_b = 3.2$ Å.

However, the theoretical curve does not express the experimental data quantitatively. The deviation is significant between $10^2 < M_w < 10^4$. Also, the theoretical curve cannot express the decrease in the slope of log $[\eta]$ against log M_w with decreasing M_w. Fujii *et al.* adopted a bond dipole moment of $\mu_{CO} = 0.99$D and a value of the characteristic ratio $C\infty = 4.0$ in benzene at 40°C to obtain the set of parameters above. This μ_{CO} value is much smaller than that derived experimentally (1.07D)[49] or calculated by a MO method[50], and we obtained a larger characteristic ratio $C\infty = 5.2$ in the present study. Therefore, the values of κ_0 and τ_0 in benzene may not be applicable to the present system.

Therefore, we tried to determine all the parameters from viscometry, by investigating the influence of the model parameters, $\lambda^{-1}\kappa_0$, $\lambda^{-1}\tau_0$, and λd_b on the shape of theoretical $M[\bar{\eta}]/\Phi_\infty L$ against L. To interpret the observed low dependence of $[\eta]$ on M_w for low M_w, the parameters set, $\lambda^{-1}\kappa_0, = 2.0 \pm 1.0$, $\lambda^{-1}\tau_0 = 4.0 \pm 1.0$, and $\lambda d_b = 0.50$ is obtained. The best fit curve (solid line) with these parameters is shown in *Figure 7*. The theoretical curve appears to explain well the experimental data for all M_w. We obtain $\log M_L/\lambda = 2.2_1$ and $\log \lambda^2 M_L = -1.6_0$, and determine $\lambda^{-1} = 18._6$ Å, $M_L = 8.7_1$ Å^{-1}, and $d_b = 9.3$ Å. The values of λ^{-1} and d_b determined are significantly bigger than those determined by Fujii *et al.*[48]. It may be noted that a relatively large hydrodynamic diameter value (9.3 Å) is obtained. We are concerned with how the hydrodynamic volume of PEO chain changes with the solvents. If one assumes that the local conformation of PEO chain does not change from that in the θ-solvent, we can determine the values of d_b, λ^{-1}, and M_L in benzene and salt-free water at 25°C. That is, we use a parameter set of $\lambda^{-1}\kappa_0 = 2.0 \pm 1.0$ and $\lambda^{-1}\tau_0 = 4.0 \pm 1.0$, determined in a θ-solvent, and compare with the $[\eta]$ values in the good solvents below $M_w = 8 \times 10^3$. The parameters determined are $d_b = 8.6$ Å, $M_L = 9.3$ Å^{-1}, and $\lambda^{-1} = 17$ Å in salt-free water at 25°C and $d_b = 5.0$ Å, $M_L = 14._5$ Å^{-1}, and $\lambda^{-1} = 16._6$ Å in benzene at 25°C. The hydrodynamic diameter in water is considerably larger than that in benzene. This may account for the fact that for $M_w < 10^4$ we observed higher $[\eta]$ in water than in benzene, as shown in *Figure 3*. Since the local conformation may vary with the solvent, the parameters determined in the good solvents may include errors. Nevertheless, it seems that the large hydrodynamic volume of PEO in water may be due to structuring waters along the PEO chain.

CONCLUSIONS

We report the aqueous solution properties of PEO in salt-free solution at 25°C and 0.45 M K_2SO_4 solution at 34.5°C. Static light scattering and viscometry measurements for PEO with M_w from 62 to 1.1×10^7 were carried out. The M_w-dependence of $\langle S^2 \rangle$ and $[\eta]$ reveals that the PEO assumes an expanded random coil conformation in water at 25°C when M_w is above $7 \sim 8 \times 10^3$. The second virial coefficient for the PEO in salt-free solution at 25°C is positive and comparable with that for PS and PMMA in good solvents. The molecular weight dependence of $[\eta]$ in the θ solvent was compared with HW model and the model parameters are determined $\lambda^{-1}\kappa_0 = 2.0 \pm 1.0$, $\lambda^{-1}\tau_0 = 4.0 \pm 1.0$, $\lambda^{-1} = 18._6$ Å, $M_L = 8.7_1$ Å^{-1}, and $d_b = 9.3$ Å. It is concluded that PEO in water behaves as a flexible polymer with a relatively large hydrodynamic diameter, compared with that in organic solvents.

ACKNOWLEDGEMENTS

The authors would like to thank Dr T. Yoshizaki, Kyoto University, for suggestions for application of the helical worklike touched-beads model to a PEO chain. The authors are also grateful to Prof. T. Kato, Mie University, for the use of the refractometer, RF-600, and Prof. T. Norisuye, Osaka University, for many valuable comments.

REFERENCES

1. Molyneux, P., ed., *Water-soluble Synthetic Polymers: Properties and Uses*. CRC Press, Boca Raton, FL, 1983.
2. Bailey, Jr. E. E. and Koleske, J. V., ed., *Alkylene Oxides and Their Polymers: Surfactant Science Series*, Vol. 35. Marcel Dekker, New York, 1991.
3. Bailey, Jr. F. E. and Koleske, J. V., *Poly(ethylene oxide)*. Academic Press, New York, 1976.
4. Stahl, G. A. and Schultz, D. N., ed., *Water-soluble Polymers for Petroleum Recovery*. Plenum Press, New York, 1988.
5. Bikales, N., ed., *Water-soluble Polymers*. Plenum Press, New York, 1973.
6. Friberg, S. E. and Lindman, B., ed., *Organized Solutions: Surfactants in Science and Technology: Surfactant Science Series*, Vol. 44. Marcel Dekker, New York, 1992.
7. Liu, K. and Parsons, J., *Macromolecules*, 1969, **2**, 529.
8. Glowinkowski, S., Jurga, K. and Pajak, Z., *Polym. Bull.*, 1981, **5**, 271.
9. Saeki, S., Kuwahara, N., Nakata, M. and Kaneko, M., *Polymer*, 1976, **17**, 685.

10. Masuhara, H. and Fukuhara, K., *J. Phys. Chem.*, 1986, **90**, 3057; 1987, **91**, 6139.
11. Masuhara, H. and Fukuhara, K., *J. Mol. Struct.*, 1985, **126**, 251.
12. Masuhara, H., Fukuhara, K. and Tamaoki, H., *J. Mol. Struct.*, 1987, **156**, 293.
13. Li, H-M., Post, B. and Morawetz, H., *Makromol. Chem.*, 1972, **154**, 89.
14. Viti, V. and Zampetti, P., *Chem. Phys.*, 1973, **2**, 223.
15. Inomata, K. and Abe, A., *J. Phys. Chem.*, 1992, **96**, 7934.
16. Tasaki, K. and Abe, A., *Polym. J.*, 1985, **17**, 641.
17. Podo, F., Nemety, G., Indovina, P. L., Radics, L. R. and Viti, V., *Mol. Phys.*, 1974, **27**, 521.
18. Smith, G. D., Yoon, D. Y. and Jafe, R. L., *Macromolecules*, 1993, **26**, 5213.
19. Polik, W. F. and Burchard, W., *Macromolecules*, 1983, **16**, 978.
20. Zhou, P. and Brown, W., *Macromolecules*, 1990, **23**, 1131.
21. Kato, T., Nakamura, K., Kawaguchi, M. and Takahashi, A., *Polym. J.*, 1981, **13**, 1037.
22. Devenand, K. and Selser, J. C., *Macromolecules*, 1991, **24**, 5943.
23. Kinugasa, S., Nakahara, H., Fudagawa, N. and Koga, Y., *Macromolecules*, 1994, **27**, 6889.
24. Lundberg, R. D., Bailey Jr. F. E. and Callard, R. W., *J. Polym. Sci., A1*, 1966, **4**, 1563.
25. Ito, K., *Macromolecular Design: Poly(ethylene oxide) Macromonomers*, ed. M. K. Mishra. Polymer Frontiers, New York, 1994.
26. Ito, K., Tomi, Y. and Kawaguchi, S., *Macromolecules*, 1992, **25**, 1534.
27. Kawaguchi, S., Winnik, M. A. and Ito, K., *Macromolecules*, 1995, **28**, 1159.
28. Kawaguchi, S., Winnik, M. A. and Ito, K., *Macromolecules*, 1996, **29**, 4465.
29. Yoshizaki, T., Nitta, I. and Yamakawa, H., *Macromolecules*, 1988, **21**, 165.
30. McGary, Jr. C. W., *J. Polym. Sci.*, 1960, **46**, 51.
31. Vink, H., *Makromol. Chem.*, 1963, **67**, 105.
32. Huggins, M. L., *J. Am. Chem. Soc.*, 1942, **64**, 2716.
33. Mead, D. J. and Fuoss, R. M., *J. Am. Chem. Soc.*, 1942, **64**, 277.
34. Pike, E. R., Pomeroy, W. R. M. and Vaughan, J. M., *J. Chem. Phys.*, 1975, **62**, 3188.
35. Beech, D. R. and Booth, C., *J. Polym. Sci., A2*, 1969, **7**, 575.
36. Miyaki, Y., Einaga, Y. and Fujita, H., *Macromolecules*, 1978, **11**, 1180.
37. Sotobayashi, H. and Springer, J., *Adv. Polym. Sci.*, 1969, **6**, 473.
38. Bailey, Jr. F. E., Kucera, J. L. and Imhof, L. G., *J. Polym. Sci.*, 1958, **32**, 517.
39. Bailey, Jr. F. E. and Callard, R. W., *J. Appl. Polym. Sci.*, 1959, **1**, 56.
40. Fujita, H., *Polymer Solutions: Studies in Polymer Science 9*. Elsevier, Amsterdam, 1990.
41. Kinugasa, S., Hayashi, H. and Hattori, S., *Polym. J.*, 1990, **22**, 1059.
42. Abe, A., Tasaki, K. and Mark, J. E., *Polym. J.*, 1985, **17**, 883.
43. Kugler, J., Fischer, E. W., Peuscher, M. and Eisenbach, C. D., *Makromol. Chem.*, 1983, **184**, 2325.
44. Vennemann, N., Lechner, M. D. and Oberthur, R. C., *Polymer*, 1987, **28**, 1738.
45. Flory, P. J., *Statistical Mechanics of Chain Molecules*. Interscience, New York, 1969.
46. Miyaki, Y., Fujita, H. and Fukuda, M., *Macromolecules*, 1980, **13**, 588.
47. Konishi, T., Yoshizaki, T. and Yamakawa, H., *Macromolecules*, 1991, **24**, 5614.
48. Fujii, M., Nagasaka, K., Shimada, J. and Yamakawa, H., *Macromolecules*, 1983, **16**, 1613.
49. Abe, A. and Mark, J. E., *J. Am. Chem. Soc.*, 1976, **98**, 6468.
50. Smith, G. D., Jaffe, R. L. and Yoon, D. Y., *J. Phys. Chem.*, 1994, **98**, 9072